

Original Research Paper

Numerical Study of Static and Dynamic Instabilities of Pinned-Pinned Pipe under Different Parameters

¹Dahmane Mouloud, ²Zahaf Samir, ³Benkhettab Mohamed and ¹Boutchicha Djilali

^{1,4}LMA, Department of Mechanical Engineering, USTO-MB, BP 1055 El Menaour, Oran 31000, Algeria

²Department of Technology, University of Djilali Bounaama-Khamis Meliana, Ain Defla-Algeria

³Department of Mechanical Engineering, Mostaganem University-Abdelhamid Ibn Badis

Article history

Received: 09-09-2020

Revised: 20-11-2020

Accepted: 21-11-2020

Corresponding Author:

Zahaf Samir

Department of Technology,

University of Djilali

Bounaama-Khamis Meliana,

Ain Defla-Algeria

Email: samir.zahaf@univ-dbk.m.dz

Abstract: In this study, the natural frequencies of the pipe transporting an fluid resting on an elastic Winkler-type and the critical velocities of instabilities are obtained by the standard finite element method. A dynamic characteristic of a pipe carrying internal fluid undergoes mechanical load due to inertia effect of fluid, Coriolis force, fluid kinetic force due to fluid flow velocity, dynamic load due to inertia effect on the pipe structure. A numerical modal analysis is realized in the fluid-structure interaction configuration. One dimensional beam finite element is used for investigating the dynamic behavior of the thin pipe. According to the approved method, the different elementary matrices were extracted, which were including to a code called Matlab. We developed a program under Matlab with R2017b version, where computations are in the complex planes. The initial approach is based on some research and analytical models. The numerical results show satisfactory agreement with the analytical results. The increase in flow velocity, mass ratio and length reduced from the rigidity of the system. Regions and range of instabilities are presented by numerical aspects. We determined the influence of the different parameters on the static and dynamic instabilities of the system.

Keywords: Pipe Conveying Fluid, Natural Frequency, Critical Velocity, Instability, Elastic Foundation, FEM, MATLAB

Introduction

The study of the subject of pipes vibrations under the internal flow is very interesting and forked. Researcher Païdoussis was able to present a book (Païdoussis and Moon, 1988) containing all his research and results, linear and non-linear equations, using analytical and experimental methods as well as factors affecting this behavior, whether geometrics and physics. The book contains more than 40 of his researches and has become a reference for every researcher in this field. Some of his research, ancient (Païdoussis and Li, 1992) and modern (Païdoussis *et al.*, 2007; Kheiri and Païdoussis, 2015), dealt with the concept of instabilities (static instability and dynamic instability). Accordingly, the researcher (Doaré and de Langre, 2000) has found new analytical formulas and that calculates the critical flow velocity inside a fixed-free tube on an elastic foundation, this was done using the Galerkin method and the same search for

the boundary conditions: Pinned-pinned and clamped-clamped (Doaré and de Langre, 2002). Then, he studied elsewhere the role of boundary conditions in the instability of one-dimensional systems (Doaré and de Langre, 2006). The importance of the subject of instability and its impact in industrial life requires a lot of research and studies. We find that (Chellapilla and Simha, 2007), studied the effect of elastic foundation Pasternak-type on the critical velocity of a fluid-conveying pipe. Same work with adoption Pasternak-Winkler model in (Chellapilla and Simha, 2008) Similar to the analytical method adopted in most of these researches (Galerkin method), there are others who used analytical method to study vibration of pipe with internal flow as differential quadrature method (Lin and Qiao, 2008), differential transformation method (Ni *et al.*, 2011) and such a generalized integral transform technique (Gu *et al.*, 2013). The aforementioned methods provided significant and valuable results, but

they remain classic and sophisticated methods, so we find researchers using numerical methods as a method of spectral element modeling in (Lee and Park, 2006) and such as finite element method (Sadeghi and Karimi-Dona, 2011; Mostafa, 2014). Dahmane *et al.* (2016) studied the pipe vibration under internal flow by calculating the natural frequencies with different parameters and they were coupled the two Commercial solvers, Fluent of fluid mechanical (CFD) and ANSYS Workbench code. The results were very impressive and satisfactory. The numerical methods that depend on the finite elements have proven to be effective in terms of results, speed in operation and easy in analysis when dealing with a coupling fluid-structure problem, see in the references (Mostafa, 2014; Dahmane *et al.*, 2016; Jiya *et al.*, 2018; Marzani *et al.*, 2012). In the present study, calculation methods have been developed for the analysis of instabilities in pinned-pinned pipe systems. Modeling of structure-fluid was conducted by the standard finite element method. So, finite element beam type with two degrees of freedom per node was used. The natural frequencies and the critical velocities of the system are calculated using a program developed on MATLAB-R2017b language. After studying the convergence and the numerical approach for our program, several examples were studied. We performed several calculations to study instability, taking into account: Fluid velocity, mass ratio, length and elastic foundation. This allows us to analyze instabilities and know factors that affect its regions and margin (range).

Vibration Equation

The problem to be considered is the free vibration analysis of a fluid-conveying pipe on an elastic foundation Winkler-model. Vibration motion equation is based on Bernoulli–Euler elementary beam theory. The physical model of pipe conveying fluid with Winkler-type is shown in “Fig. 1”. “Figure 2a” shows forces on fluid element while, “Fig. 2b” shows forces and moment of pipe element. The pipe is long and straight L conveying an incompressible fluid, where U is mean velocity; the motions are small ($dX \approx \delta s$), “Fig. 2a”. The pipe rests on an elastic foundation Winkler-type soil of modulus K , “Fig. 1”. In the “Fig. 2”, m_s and m_f masses per unit length of the incompressible fluid and the structure, respectively. The Boundary conditions for pinned-pinned pipe are:

$$Y|_{x=0} = \frac{\partial^2 y}{\partial X^2}|_{x=0} = Y|_{x=L} = \frac{\partial^2 y}{\partial X^2}|_{x=L} = 0 \quad (1)$$

The equation for conveying pipe carrying fluid on a Winkler elastic foundation is given as (Paidoussis and Moon, 1988):

$$EI \frac{\partial^4 Y}{\partial X^4} + m_f U^2 \frac{\partial^2 Y}{\partial X^2} + 2m_f U \frac{\partial^2 Y}{\partial X \partial T} + (m_s + m_f) \frac{\partial^2 Y}{\partial T^2} + KY = 0 \quad (2)$$

The “Equation (1)” is a fourth-order partial differential equation in two independent variables subject to various boundary conditions.

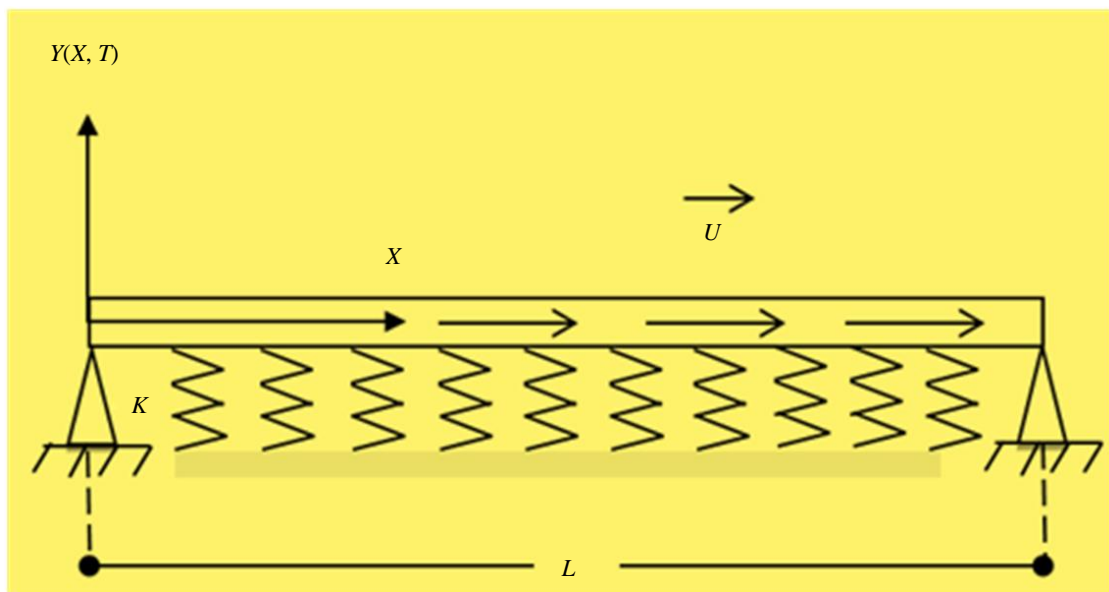


Fig. 1: Representation of the pipe-conveying fluid resting on an elastic Winkler-type

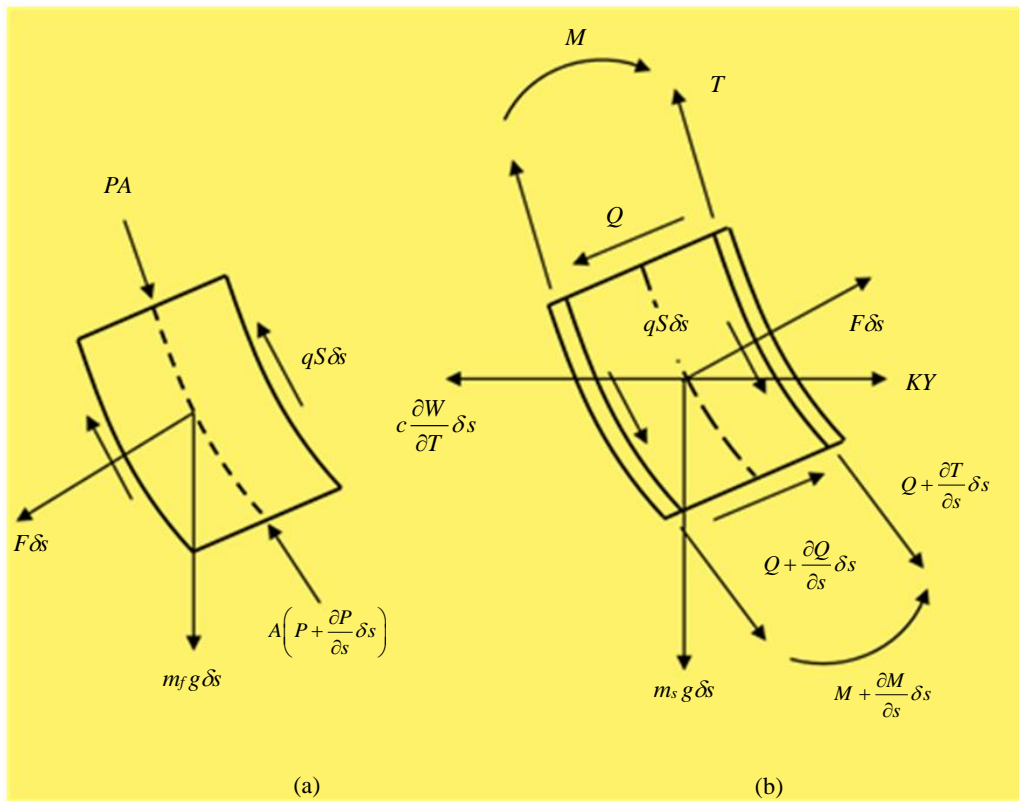


Fig. 2: (a) Forces on fluid element; (b) forces and moments on pipe element δs (Paidoussis and Moon, 1988)

Finite Element Discretization

The equation of element deflection for straight one-dimensional beam elements could have the form (Rao, 2017; 2011):

$$W(X,T) = \sum_{i=1}^N N_i(X)W_i(T) \tag{3}$$

where:

- $[N_i]$ = Represent the shape function
- $W_i(T)$ = The function which represents the displacements shape, “Equation (4)” and, rotation at the nodes, “Equation (5)”

The “Equation (3)” becomes:

$$W(X,T) = N_1(X)W_1(T) + N_2(X)\theta_1(T) + N_3(X)W_2(T) + N_4(X)\theta_2(T) \tag{4}$$

And:

$$\theta(X,T) = N'_1(X)W_1(T) + N'_2(X)\theta_1(T) + N'_3(X)W_2(T) + N'_4(X)\theta_2(T) \tag{5}$$

Shape functions:

$$\begin{cases} N_1 = 1 - 3\frac{N^2}{N^2} + 2\frac{N^3}{N^3} \\ N_2 = X - 2\frac{N^2}{N} + \frac{X^3}{N^2} \\ N_3 = 3\frac{N^2}{N^2} - 2\frac{N^3}{N^3} \\ N_4 = \frac{N^3}{N^2} - \frac{N^2}{N} \end{cases} \tag{6}$$

Elementary Matrices

Using the energy principle (Rao, 2017; Zhai *et al.*, 2011), where the potential (deformation) energy of the solid element can be expressed:

$$V_s = \frac{1}{2} \int_0^L EI \left(\frac{d^2W}{dX^2} \right)^2 dX \tag{7}$$

And the kinetic energy of the solid element can be expressed:

$$T_s = \frac{1}{2} \int_0^L ms \frac{d^2W}{dT^2} dX \tag{8}$$

The kinetic energy of the fluid element can be expressed by (Mostafa, 2014; Marzani *et al.*, 2012):

$$T_f = \frac{1}{2} \int m_f \left(U \frac{dW}{dX} + \frac{dW}{dT} \right)^2 dX \quad (9)$$

The potential energy over the length of elastic foundation can be expressed by (Mostafa, 2014; Jiya *et al.*, 2018):

$$V = \frac{1}{2} \int_0^L KW^2 dX \quad (10)$$

$$[K_s] = \frac{m_f U^2}{30L} \begin{bmatrix} 12 & 6L & -12 & 6L \\ 6L & 4L^2 & -6L & 2L^2 \\ -12 & -6L & 12 & -6L \\ 6L & 2L^2 & -6L & 4L^2 \end{bmatrix} \quad (11)$$

$$[K_f] = \frac{m_f U^2}{30L} \begin{bmatrix} 36 & 3L & -36 & 3L \\ 3L & 4L^2 & -3L & -L^2 \\ -36 & -3L & 36 & -3L \\ 3L & 3L^2 & -3L & 4L^2 \end{bmatrix} \quad (12)$$

$$[M] = \frac{(m_s + m_f)L}{420} \begin{bmatrix} 156 & 22L & 54 & -13L \\ 22L & 4L^2 & 13L & -3L^2 \\ 54 & 13L & 156 & -22L \\ -13L & -3L^2 & -22L & 4L^2 \end{bmatrix} \quad (13)$$

$$[C] = \frac{2m_f U}{30} \begin{bmatrix} -30 & 6L & 30 & -6L \\ -6L & 0 & 6L & -L^2 \\ -30 & -6L & 30 & 6L \\ 6L & L^2 & -6L & 0 \end{bmatrix} \quad (14)$$

$$[F] = \frac{KL}{420} \begin{bmatrix} 156 & 22L & 54 & -13L \\ 22L & 4L^2 & 13L & -3L^2 \\ 54 & 13L & 156 & -22L \\ -13L & -3L^2 & -22L & 4L^2 \end{bmatrix} \quad (15)$$

where, $[K_s]$, $[K_f]$, $[M]$, $[C]$ and $[F]$ respectively, the structure stiffness, the fluid stiffness, the masses, the damping and the foundation matrices of the system.

The Natural Frequencies

After using the Lagrange principle (Dahmane *et al.*, 2020a), the equation of motion by finite element method is:

$$[M]\{\ddot{q}\} + [C]\{\dot{q}\} + ([K])\{q\} = 0 \quad (16)$$

where, $[K]$ is the rigidity (global stiffness) of the system:

$$[K] = [K_s] - [K_f] \quad (17)$$

The solution of Equation (16) is very complicated with presence of damping, so we use the variable change method (state-space):

$$E\dot{z} + Gz = 0 \quad (18)$$

where the state variable is:

$$z = \begin{Bmatrix} \dot{q} \\ q \end{Bmatrix} \quad (19)$$

The matrices $[E]$ and $[G]$ are calculated through variable-change as the following:

$$E = \begin{bmatrix} M & 0 \\ 0 & K \end{bmatrix} \quad (20)$$

$$G = \begin{bmatrix} C & K \\ -K & 0 \end{bmatrix} \quad (21)$$

If, the solution of Equation (16) is taken as:

$$\{q\} = \{E\} \cdot \exp(\lambda t) \quad (22)$$

In addition, λ is eigenvalues of the system and the $\{E\}$ corresponding eigenvectors of this value:

$$\lambda = \omega j \quad (23)$$

In addition, the solution of equation is sought in the general form:

$$z = \begin{Bmatrix} \lambda \{E\} \\ \{E\} \end{Bmatrix} \exp(\lambda t) = \{E\} \exp(\lambda t) \quad (24)$$

The system equation of government can be transformed from state space by:

$$\left\{ \begin{bmatrix} 0 & I \\ -M^{-1}K & -M^{-1}C \end{bmatrix} - \lambda \begin{bmatrix} I & 0 \\ 0 & I \end{bmatrix} \right\} \begin{Bmatrix} \lambda \{E\} \\ \{E\} \end{Bmatrix} = \begin{Bmatrix} 0 \\ 0 \end{Bmatrix} \quad (25)$$

I is a unity matrix.

We ask ourselves:

$$H = \begin{bmatrix} 0 & I \\ -M^{-1}K & -M^{-1}C \end{bmatrix} \quad (26)$$

Eigenvalues are complex; they give in the form:

$$\lambda^m = Re^m + j\omega^m \quad (27)$$

Re : The real part of the eigenvalue and is the damping of the system

Ω : The imaginary part of the Eigen value, is therefore the proper pulsation of our system

The characteristics of the roots are obtained here, using the Matlab code (Dahmane *et al.*, 2020b).

We introduce the non-dimensional variables and parameters:

$$x = X / L, y = Y / L, t = \left(EI / (m_f + m_s) \right)^{1/2} T / L^2,$$

$$\beta = m_f / (m_f + m_s),$$

$$u = UL (m_f / EI)^{1/2}, k = KL^2 / EI$$

Numerical Results

This research seeks to study the two types of instabilities and this comes by calculating the two critical velocities in the static pattern (buckling) and the dynamic pattern (flutter), that accompanies the disappearance of the first natural frequency in both cases. Results will be discussed for various values of flow velocity, mass ratio, length L and elastic foundation for pinned-pinned pipes. The physical parameters as: Elastic modulus of structure is (211 GPa); incompressible fluid (H_2O), density is (1000 kg/m^3); elastic structure (pipe), density is (7850 kg/m^3). The geometrical parameters as: Pipe length is ($1 \div 2 \text{ m}$); the thickness corresponds β belongs to [$0.1, 0.6$]; outer diameter of the pipe is (0.03 m).

Instability study mainly depends on calculating the first frequencies of the tube structure under the influence of pressure resulting from increasing flow velocities, passing through the first critical velocity where the resulting force are identical to the so-called buckling (static instability). This stage continues for a period of time (instability range) that coincides with absence of the first mode of vibration, up to the second critical velocity that corresponds to dynamic instability (flutter).

Along the static instability range, the structure passes from linear to non-linear, where the system suffers from severe fatigue. So, our research deals with the study of the transition period between static instability and dynamic instability.

The cases can be divided into three according to the parameters effect (masse ratio, length and elastic foundation). In the case one, firstly the convergence was performed for a velocity $U = 100 \text{ m/s}$, 15 elements have been adopted, 13 elements are sufficient for three first modes Fig. 3.

The numerical results are obtained by DTM and FEM for masse ratio $\beta = 0.1$. The results obtained are similar, Fig. 4.

The same study for $\beta = 0.3$ and $\beta = 0.5$ with the adoption of the numerical method. Figures 5 and 6 shows these calculations. These figures present almost the same natural frequencies and the same first critical velocity; this what many researchers believe [1, 9], but the physic (dimensional) results show variations in values and this is what we see in the following figure. So, the Fig. 7 shows the physical results accompanying the non-dimensional results in the Figs. 5 and 6 for $\beta = 0.3$ and $\beta = 0.5$, respectively.

For $U \equiv 0$ (very low velocity), the variation for the first frequency is 12%, it is the same for both other frequencies. For $U \equiv U_{cr}$, the variation between the two states is equal 30%, whereas the critical velocity is reduced with 33% corresponding to the dynamic instability (flutter).

The variation for instability static range is 33%. This means that raising the value of β weakens the structure rigidity, which leads to decrease natural frequencies and, of course, critical velocities. Part of this variation is shown in the previous figures in the use of the number of iterations in terms of velocity, so that it is more severe in Fig. 4 compared to the two that followed.

From another perspective, these big variations are caused by the passage of a large amount of fluid that generates Coriolis forces by positive damping, which grows with time, leading to a decrease in system rigidity and consequently the frequencies.

The Figs. 8 and 9 shows the action of this damping effect, which is manifested in the form of real part of the first natural frequency where $\beta = 0.3$ and fluid velocity is limited to the field [0.8].

The second case, we calculated the first three natural frequencies as a function of the fluid velocity for three different lengths ($L = 1, L = 1.5, L = 2$), Figs. 10 and 11 in order to study its effect on instability of both types. So, the Fig. 12 represents the variations for two mass ratios.

The variations show that length has significant effect on the rigidity, which lowers the frequencies of the system according to the fluid velocity and consequently quickly reaches the first critical velocity of buckling. The biggest variation here is equal to 44%. The change in the level of instability range is evident, increasing with the increase in length. The Fig. 12 shows critical velocities (static part) of pinned-pinned pipe as function of the masse ratio in the field [0.6] for different lengths. The results show that the critical velocity of flow diminishes as the length parameter increases.

Mass Ratio Effect

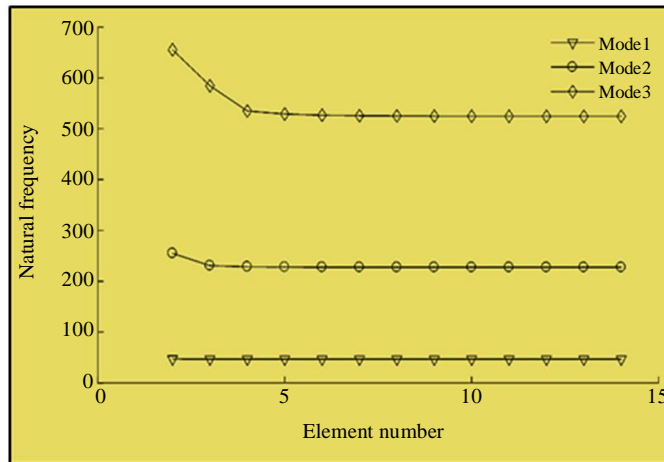


Fig. 3: Convergence of the first three natural frequencies of pinned-pinned pipe conveying fluid, with $U = 100$ m/s, $\beta = 0.5$

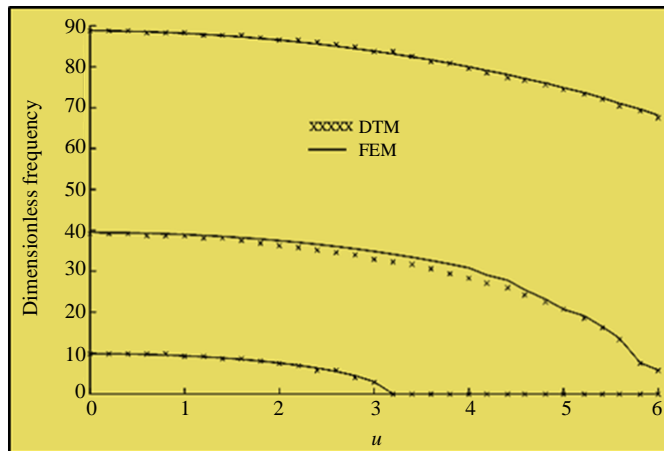


Fig. 4: Dimensionless frequency for various values of u , for the lowest three modes of a pipe conveying fluid, DTM (Ni *et al.*, 2011) (xxx) and FEM (\rightarrow), $\beta = 0.1$

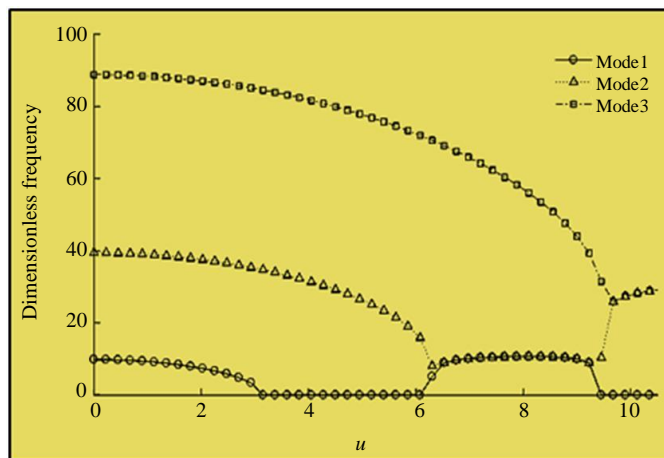


Fig. 5: Dimensionless frequency for various values of u , for the lowest three modes of a pipe conveying fluid, $\beta = 0.3$

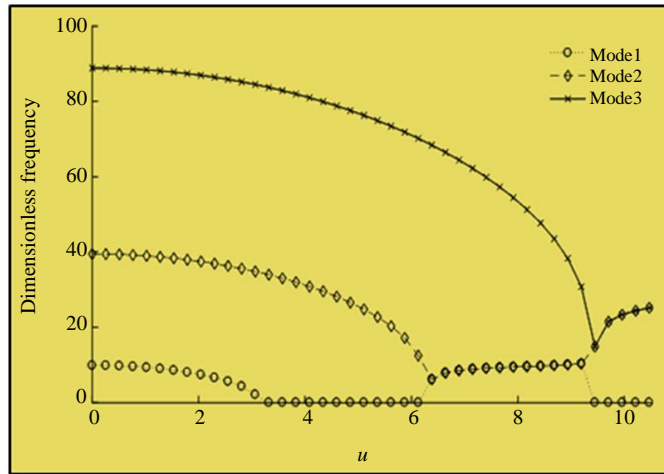


Fig. 6: Dimensionless frequency for various values of u , for the lowest three modes of a pipe conveying fluid, $\beta = 0.5$

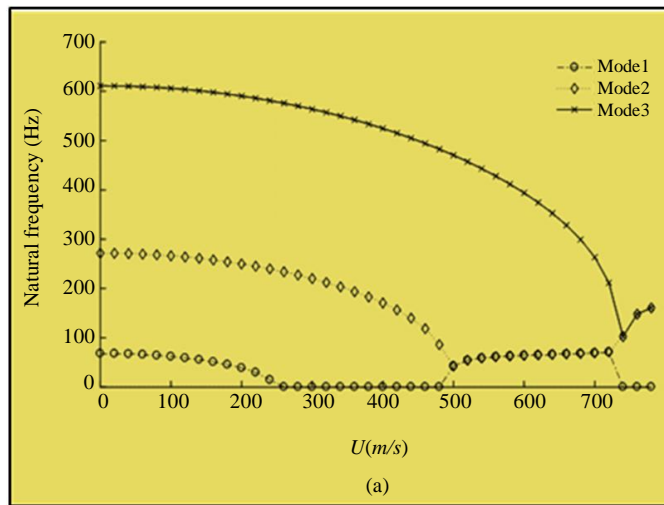


Fig. 7: Three proper modes on fluid velocity function of pinned-pinned pipe conveying fluid, (a) $\beta = 0.3$

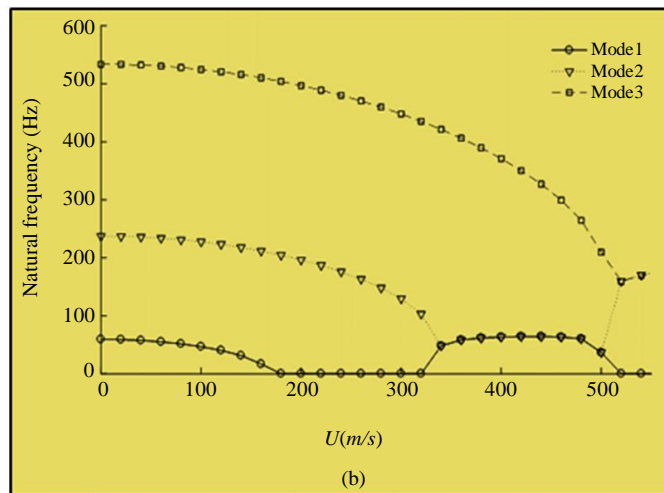


Fig. 8: Three proper modes on fluid velocity function of pinned-pinned pipe conveying fluid, (b) $\beta = 0.5$

Elastic Foundation Effect

The final case of this research deals with the study of the elastic foundation on system instabilities. Table 1 presents the critical velocities for static instability of the pinned-pinned pipe as functions of the foundation stiffness k , with $\beta = 0.5$.

The variation in results is evident, especially for high Winkler parameter. The “Fig. 13” shows elastic foundation effect ($k = 10^3$) on the variation of the first modes as a function of the fluid velocity. Compared to the first case ($k = 0$), we find that the largest variation in the frequency values is equal to 70%, while the

instability range lowers by 36% and the critical velocity that corresponds to dynamic instability is 9.859.

Table 1: The critical velocity parameter for various values of Winkler-model (k)

k values	Critical velocity	Variation %
0.1	3.142	0.12
1	3.158	1.60
10	3.298	4.43
100	4.472	35.59
200	5.489	22.74
300	6.348	15.64
400	7.049	11.04
500	7.226	2.51
1000	8.0596	11.53

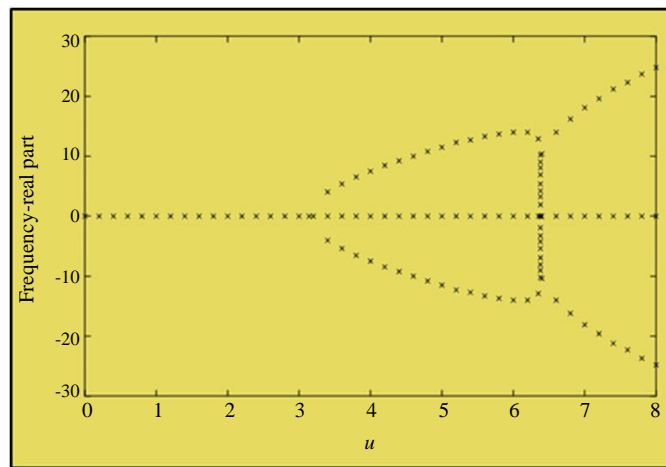


Fig. 9: Real part of the first Eigen mode as function of fluid velocity

Length Effect

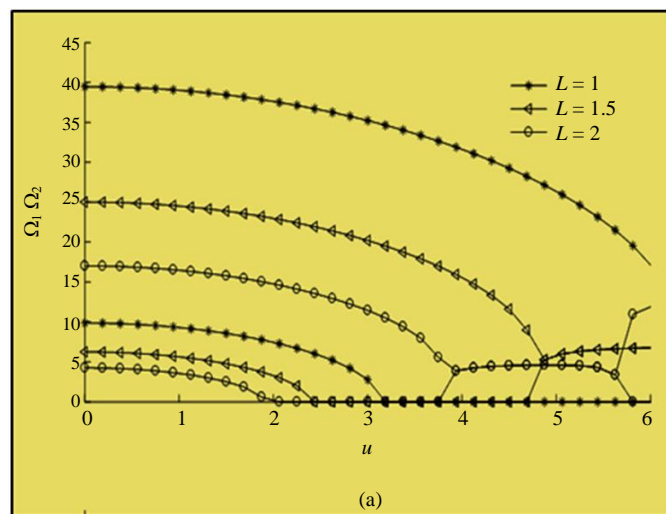


Fig. 10: Two proper modes on fluid velocity function of pinned-pinned pipe conveying fluid for different length, (a) $\beta = 0.3$, (b) $\beta = 0.5$

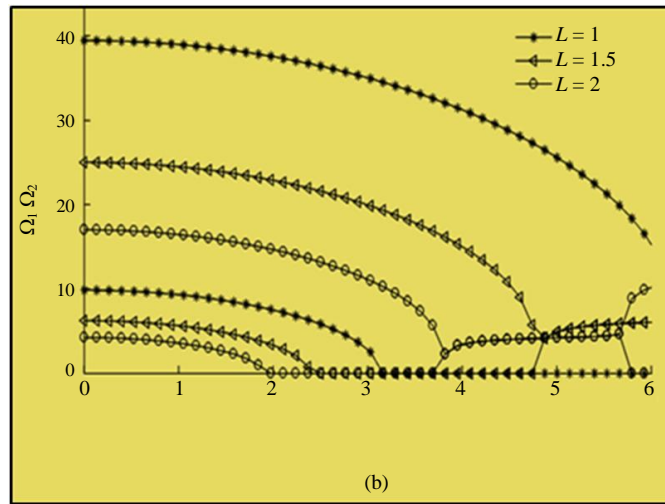


Fig. 11: Two proper modes on fluid velocity function of pinned-pinned pipe conveying fluid for different length, (b) $\beta = 0.5$

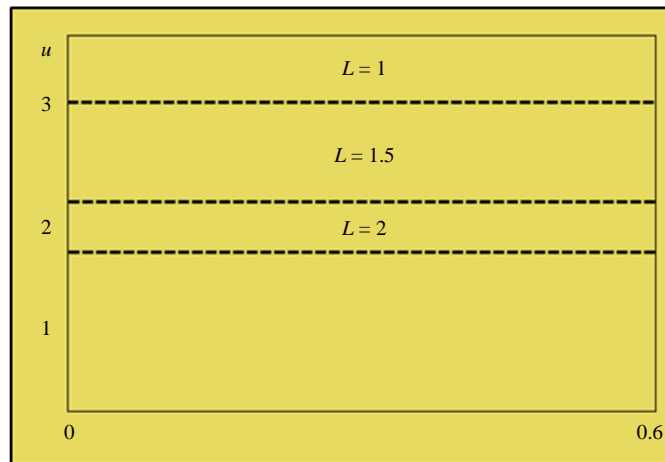


Fig. 12: Critical velocities of pinned-pinned pipe as function of the masse ratio for different lengths

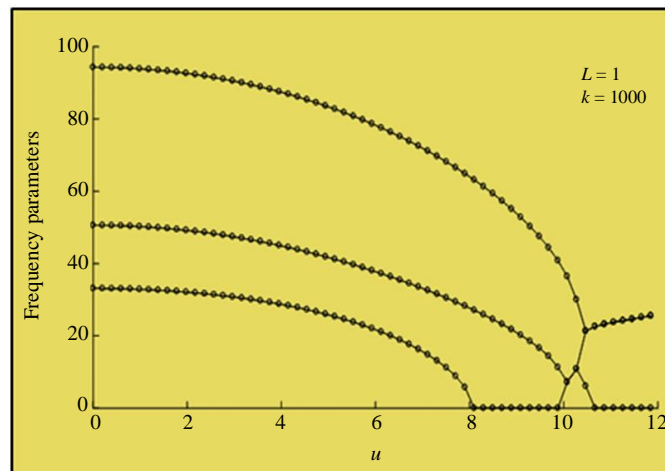


Fig. 13: Effect of foundation stiffness on the natural frequency of the pinned-pinned pipe at different fluid velocities, $\beta = 0.5$

Conclusion

In this study, we have studied the instabilities of pinned-pinned pipe carrying incompressible fluid. The numerical aspect with the finite method gives solutions in a complex plane by determining the Eigen modes. Numerical results give the natural frequencies and critical velocity that characterized instabilities. Several examples were processed to determine the influence of the fluid flow velocity and different physical and geometrical parameters on the phenomenon of fluid-structure interaction. The main findings can be summarized as follows:

1. The first conclusion which one can draw from this study is that the frequencies of the system fluid-structure depend on the physical and geometrical factors
2. We observe that instability appears when the velocity exceeds a threshold called critical velocity of instability, when the first proper mode is zero
3. The results obtained numerically are similar to those obtained by the semi-analytical method for the determination of the first natural frequencies
4. We have noticed that increasing β slightly decreases the natural frequencies of the system and consequently decreases their critical velocities
5. The length parameter decreases the frequencies and critical fluid velocities and leads to an increase in the instability margin
6. Winkler elastic foundation increases the natural frequencies of the system and consequently the critical velocities, while the range of static instability is decreasing. What distinguishes most of this research from others is its discussion of the axis of instability and what it means in this field that is why we did some analysis and calculation in this research, hoping to continue with other work in the same field

Acknowledgement

Thanks to group members who contribute in this research from the first one to the last.

Author's Contributions

All authors equally contributed in this study.

Ethics

This article is original and contains unpublished material. The corresponding author confirms that all of the other authors have read and approved the manuscript and no ethical issues involved.

References

- Chellapilla, K. R., & Simha, H. S. (2007). Critical velocity of fluid-conveying pipes resting on two-parameter foundation. *Journal of sound and vibration*, 302(1-2), 387-397.
- Chellapilla, K. R., & Simha, H. S. (2008). Vibrations of fluid-conveying pipes resting on two-parameter foundation. *The Open Acoustics Journal*, 1(1).
- Dahmane, M., Boutchicha, D., & Adjlout, L. (2016). One-way fluid structure interaction of pipe under flow with different boundary conditions. *Mechanics*, 22(6), 495-503.
- Dahmane, M., Samir, Z., Mawhoub, S., Sid Ahmed, S., Benkhettab M., & Djilali, B., (2020a). Numerical study of post-buckling of clamped-pinned pipe carrying fluid under different parameters. *Current Research in Bioinformatics*, 9, 35-44.
- Dahmane, M., Boutchicha, D., & Benkhettab, M., (2020b). Méthode numérique-programme en MATLAB. 108-115.
- Doaré, O., & de Langre, E. (2000, June). Local and global instability of fluid-conveying cantilever pipes.
- Doaré, O., & de Langre, E. (2002). Local and global instability of fluid-conveying pipes on elastic foundations. *Journal of fluids and structures*, 16(1), 1-14.
- Doaré, O., & de Langre, E. (2006). The role of boundary conditions in the instability of one-dimensional systems. *European Journal of Mechanics-B/Fluids*, 25(6), 948-959.
- Gu, J., An, C., Duan, M., Levi, C., & Su, J. (2013). Integral transform solutions of dynamic response of a clamped-clamped pipe conveying fluid. *Nuclear Engineering and Design*, 254, 237-245.
- Jiya, M., Inuwa, Y. I., & Shaba, A. I. (2018). Dynamic response analysis of a uniform conveying fluid pipe on two-parameter elastic foundation. *Science World Journal*, 13(2), 1-5.
- Kheiri, M., & Païdoussis, M. P. (2015). Dynamics and stability of a flexible pinned-free cylinder in axial flow. *Journal of Fluids and Structures*, 55, 204-217.
- Lee, U., & Park, J. (2006). Spectral element modelling and analysis of a pipeline conveying internal unsteady fluid. *Journal of fluids and structures*, 22(2), 273-292.
- Lin, W., & Qiao, N. (2008). In-plane vibration analyses of curved pipes conveying fluid using the generalized differential quadrature rule. *Computers & structures*, 86(1-2), 133-139.
- Marzani, A., Mazzotti, M., Viola, E., Vittori, P., & Elishakoff, I. (2012). FEM formulation for dynamic instability of fluid-conveying pipe on nonuniform elastic foundation. *Mechanics based design of structures and machines*, 40(1), 83-95.

Mostafa, N. H. (2014). Effect of a Viscoelastic foundation on the Dynamic Stability of a Fluid Conveying Pipe. *International Journal of Applied Science and Engineering*, 12(1), 59-74.

Ni, Q., Zhang, Z. L., & Wang, L. (2011). Application of the differential transformation method to vibration analysis of pipes conveying fluid. *Applied Mathematics and Computation*, 217(16), 7028-7038.

Paidoussis, M. P., & Li, G. X. (1992). Cross-flow-induced chaotic vibrations of heat-exchanger tubes impacting on loose supports. *Journal of Sound and Vibration*, 152(2), 305-326.

Paidoussis, M. P., & Moon, F. C. (1988). Nonlinear and chaotic fluidelastic vibrations of a flexible pipe conveying fluid. *Journal of Fluids and Structures*, 2(6), 567-591.

Païdoussis, M. P., Semler, C., Wadham-Gagnon, M., & Saaid, S. (2007). Dynamics of cantilevered pipes conveying fluid. Part 2: Dynamics of the system with intermediate spring support. *Journal of Fluids and Structures*, 23(4), 569-587.

Rao, S. S. (2011). *Mechanical vibrations*. 5th ed, Prentice Hall.

Rao, S. S. (2017). *The finite element method in engineering*. Butterworth-heinemann.

Sadeghi, M. H., & Karimi-Dona, M. H. (2011). Dynamic behavior of a fluid conveying pipe subjected to a moving sprung mass—an FEM-state space approach. *International Journal of Pressure Vessels and Piping*, 88(4), 123-131.

Zhai, H. B., Wu, Z. Y., Liu, Y. S., & Yue, Z. F. (2011). Dynamic response of pipeline conveying fluid to random excitation. *Nuclear Engineering and Design*, 241(8), 2744-2749.

Nomenclature

x	: Cartesian coordinate
y	: Cartesian coordinate
u	: Velocity
U	: Velocity of fluid
t	: Time
P	: Pressure
M	: Moment of inertia
m	: Mass
δ	: Pipe element
m_s	: Mass per unit length
m_f	: Mass per unit of a conveying fluid
EI	: Flexural rigidity
A	: Cross- section area
L	: Length of pipe
k	: Dimensionless winkler foundation
β	: Mass ration
E	: Elastic modulus of pipe